ADNI Progress report

Devendra Goyal
Uniqname: devendra

November 14, 2014

Part I

Using HMMs to predict disease progression

1 Statistics about the data

There are several choices here for the dataset to be used:

- One of MRI/PET/CSF only
- Some combination of 2/3 available modalities
- Use all three modalities
- Add demographics data to any of the above options

For now, I have decided to use only the FDG-PET data for the HMM problem.

The pros are:

- The PET data is the cleanest and most easy dataset to process.
- The feature space is relatively low dimensional. It is the

$$mean, median, mode, min, max, stdev$$

of the glucose expression for 5 expert defined regions in the brain - making it a total of 30 features for each patient.

- Don't have to deal with failed segmentation amongst patients, or missing variables. This dataset was processed by the latest available package in the field, and the lab releasing it has cleaned it perfectly for plug-and-play use.
- The pre-processing for PET scans accross all ADNI cohorts (ADNI1, ADNIGO, ADNI2) was done in one go by the same group using the same software, guaranteeing us homogenity in the data.

The cons are:

- Throwing away a lot of useful information from MRIs, CSFs, demographics
- A small number of patients (= 720) have more than one PET scan (accross all cohorts), which could making learning the HMM a problem

Some possible solutions for the future:

- It is potentially a very interesting problem to think about the use of observations from multiple modalities in a HMM setting. The reason this is better than doing it in an SVM setting is - due to the generative nature of the HMMs, we do not have to throw away patients who have missing observations for any of the three modalities.
- For the same reason as above, it will be interesting to think about the problem of dealing with missing data.

There are a total of 1404 patients accross all three cohorts with PET data, out of which only 1398 have baseline diagnoses. Out of those, only **720 patients** have more than one visit. The distribution for these patients is as follows:

	NL	MCI			AD
		MCI-c	MCI-nc	MCI-rev	
FDG-PET	225	126	237	30	102

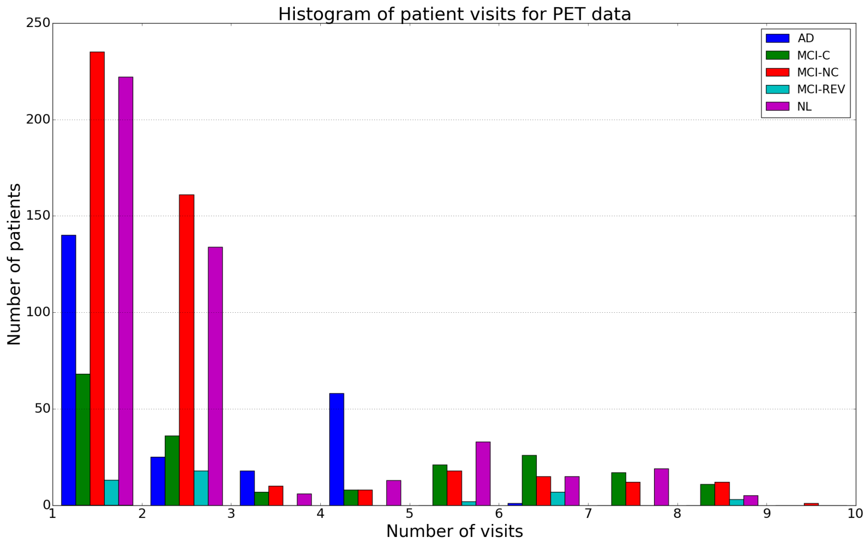

Figure 1: Diagnoses of patients who had usable PET scans

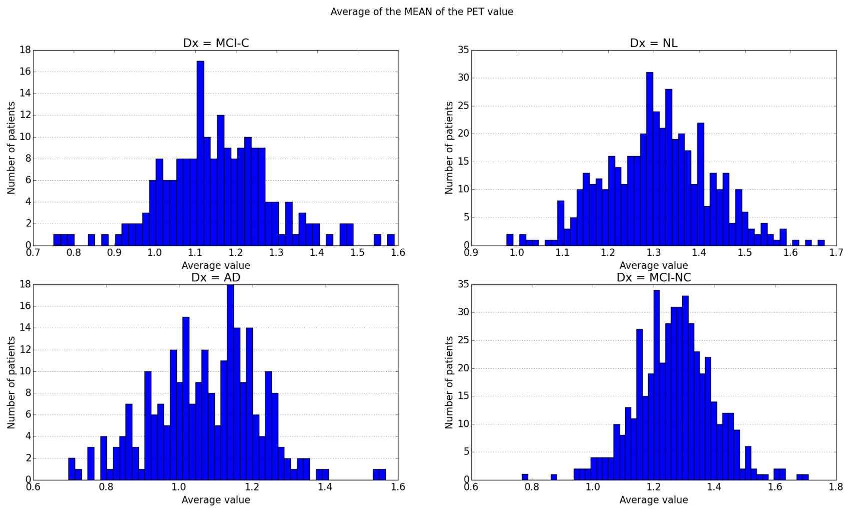

Figure 2: Histograms of the MEAN of FDG scans for different diagnoses

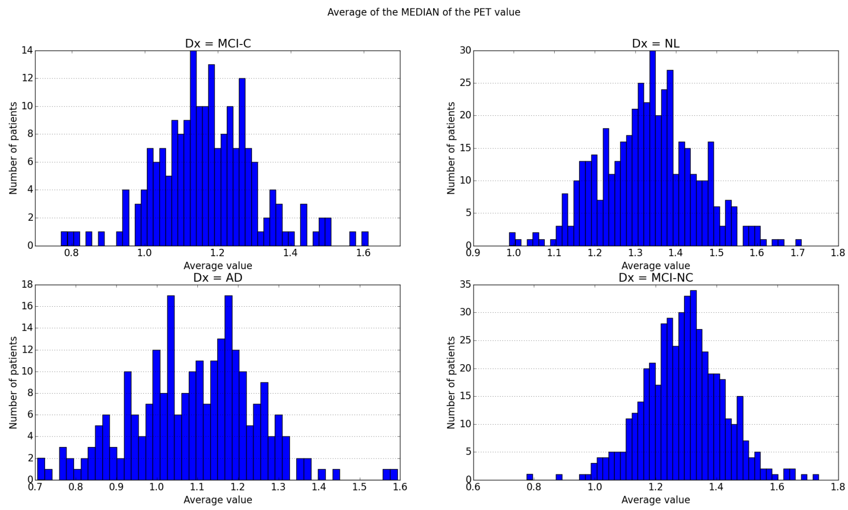

Figure 3: Histograms of the MEDIAN of FDG scans for different diagnoses

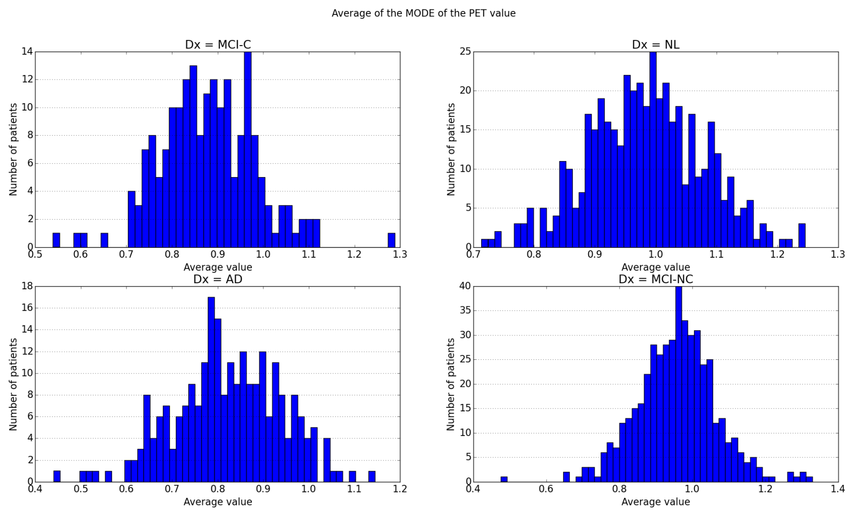

Figure 4: Histograms of the MODE of FDG scans for different diagnoses

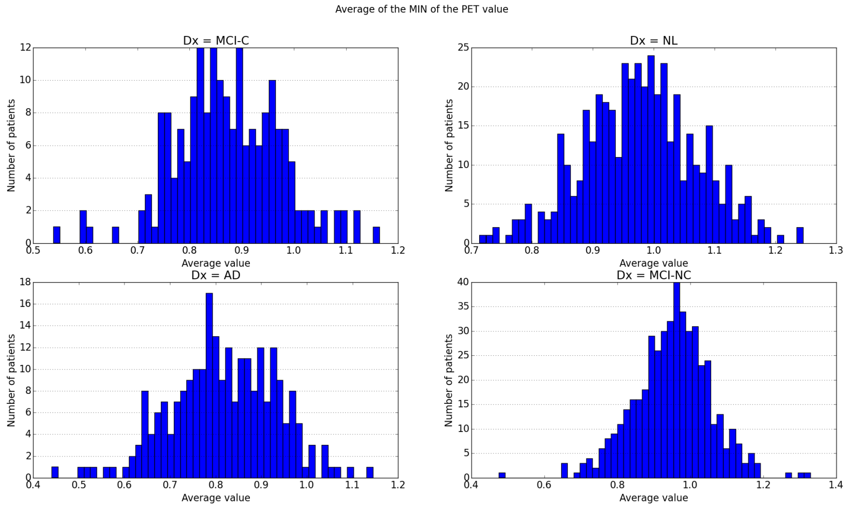

Figure 5: Histograms of the MIN of FDG scans for different diagnoses

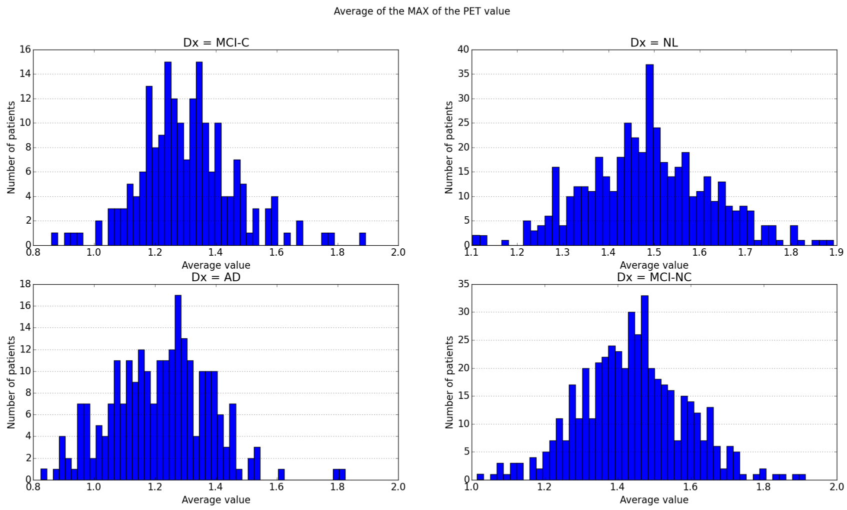

Figure 6: Histograms of the MAX of FDG scans for different diagnoses

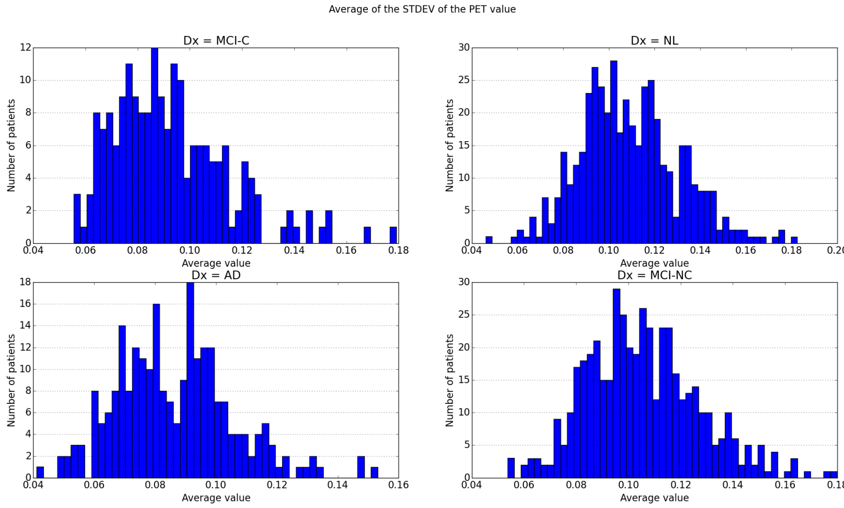

Figure 7: Histograms of the STDEV of FDG scans for different diagnoses

Shown below are histograms to depict the distribution of patients having varying number of visits. Note that for cases where the histogram shows patients having data from two different sources, only cases where the data occurs from the **same visit** is considered.

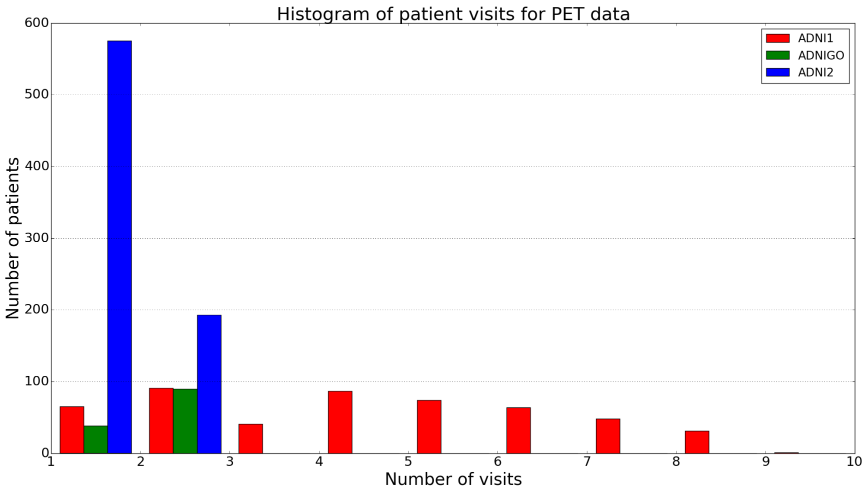

Figure 8: Distribution of patients who had PET scans

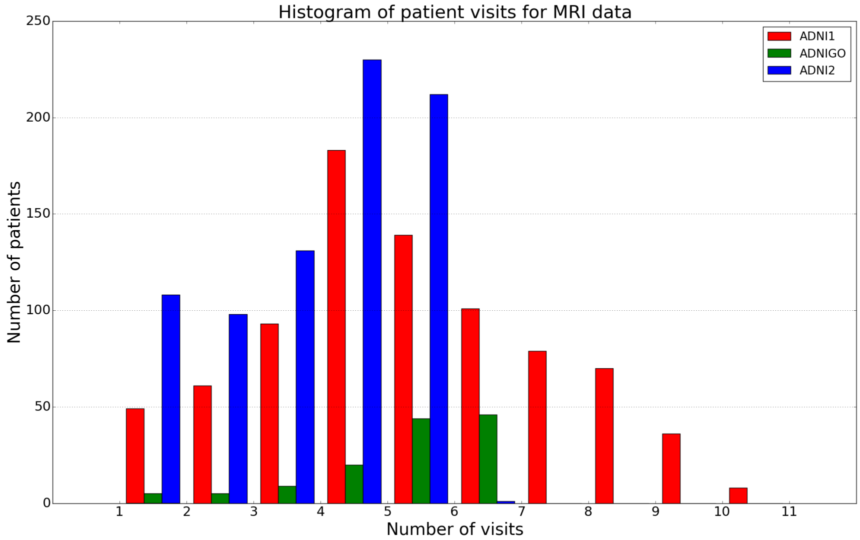

Figure 9: Distribution of patients who had MRI scans

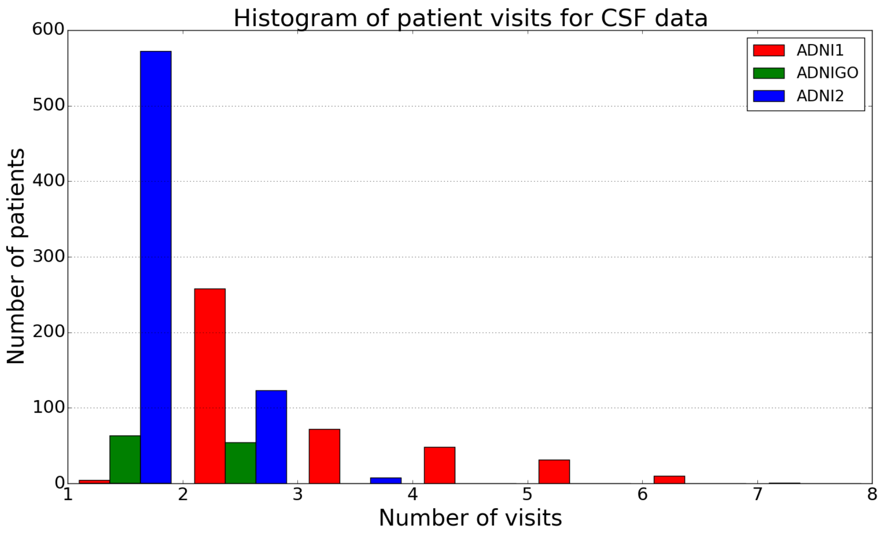

Figure 10: Distribution of patients who had CSF data

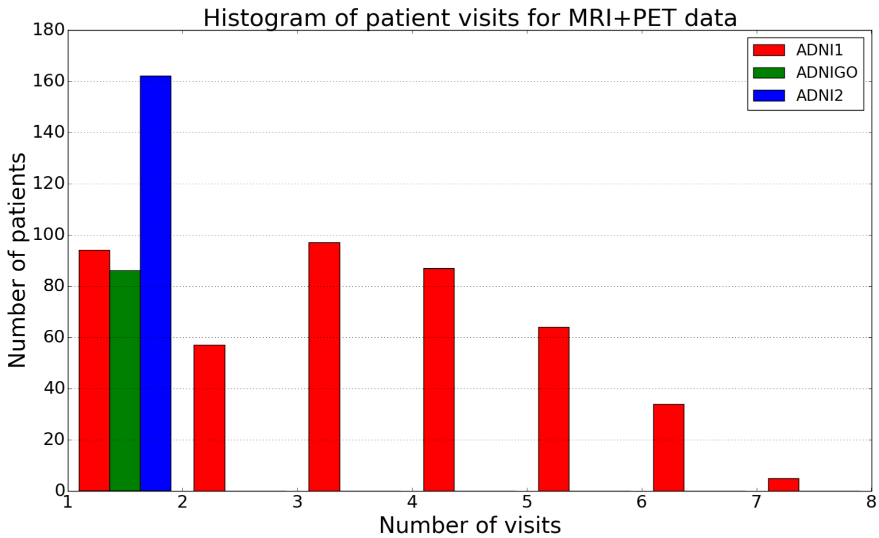

Figure 11: Distribution of patients who had MRI+PET scans

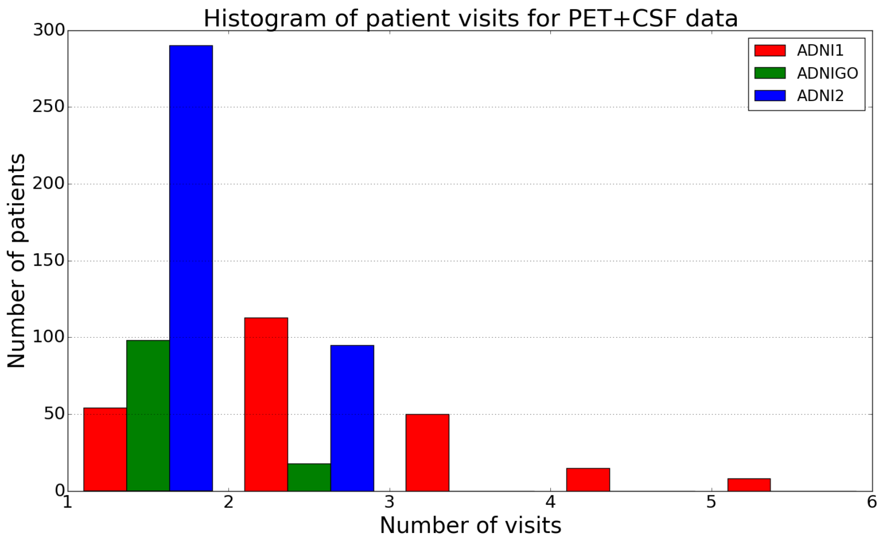

Figure 12: Distribution of patients who had PET+CSF data

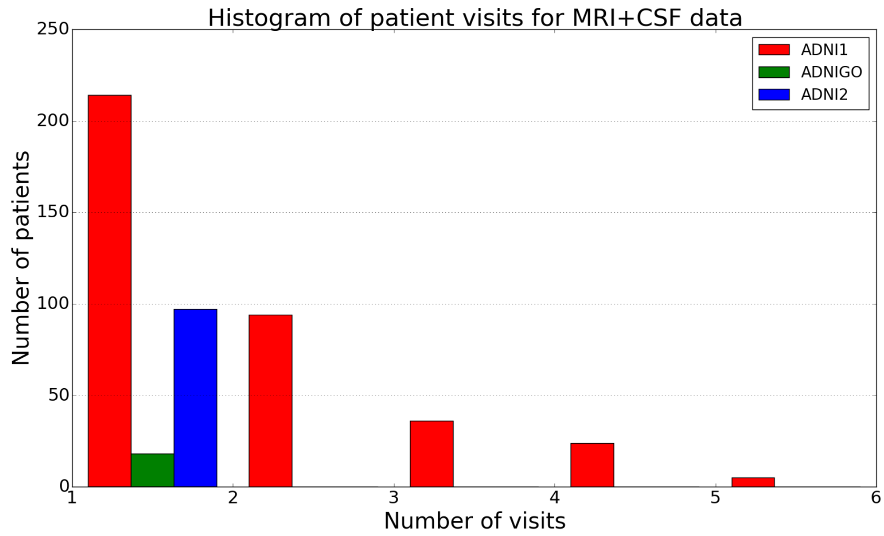

Figure 13: Distribution of patients who had MRI+CSF data

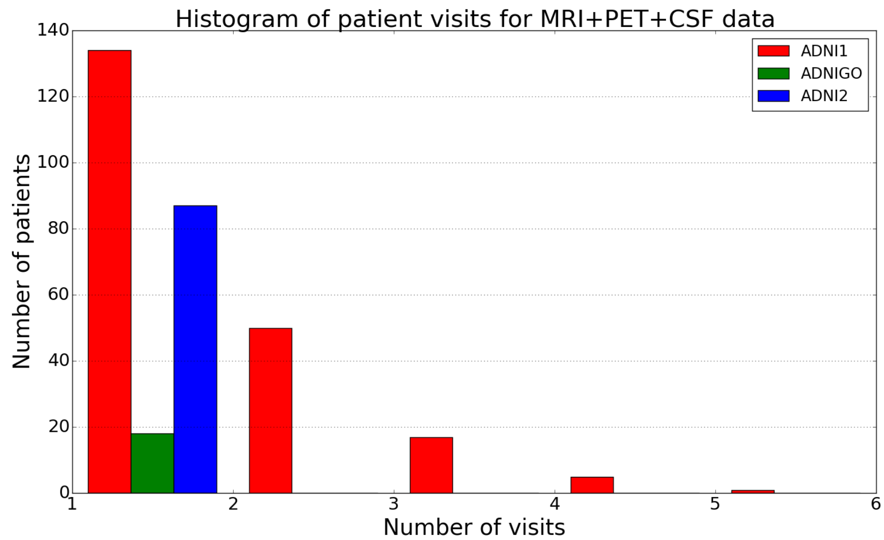

Figure 14: Distribution of patients who had MRI+PET+CSF data

Part II

Establishing the baseline

2 Statistics about the Data

The results shown in this document are based on the ADNI-1 cohort. There are several pros and cons of this decision:

2.1 Pros

- All the pre-processed features uploaded on the ADNI website operate on the entire cohort, thus there is homogeneity in terms of the features available for each patient across each modailty. MRI images for ADNI-GO/2 have been processed using different versions of the same software, and are also collected using a higher resolution MRI machine. While this is not a dealbreaker per se, it will require significantly more work to process all the images using the same software and generate similar features.
- Most of the recent literature (5 years) relies on data from ADNI1 only to report results. This will give us a chance to compare our results directly with some of these reported results.
- ADNI-1 is the best dataset to track patients longitudinally, as it was started in 2004 and we have about 8 years' worth of data for all MCI and AD patients that the protocol chose to follow (more on this later).

2.2 Cons

- ADNI1 has CSF data available for only about 20% of the patients. This number will become even smaller when we look at the number of patients that have data available for all 3 modalities.

Below is a chart summarizing the study design:

The table below summarizes the numbers for the **ADNI1** cohort only, for the MRI and PET modalities.

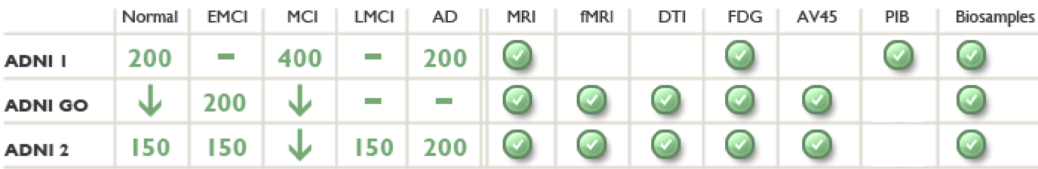

	Normal	EMCI	MCI	LMCI	AD	MRI	fMRI	DTI	FDG	AV45	PIB	Biosamples
ADNI 1	200	–	400	–	200	✓			✓		✓	✓
ADNI GO	↓	200	↓	–	–	✓	✓	✓	✓	✓		✓
ADNI 2	150	150	↓	150	200	✓	✓	✓	✓	✓		✓

Figure 15: ADNI study design

	NL	MCI			AD
		MCI-c	MCI-nc	MCI-rev	
FDG-PET	102	94	96	13	97
MRI(clean)	180	133	132	10	123
MRI(complete)	229	196	183	18	192
FDG+MRI(clean)	79	66	68	9	62
FDG+MRI(complete)	102	94	96	13	97

3 SVMs on classification task

All of the following classification results are based only on features evaluated for the patients at **baseline**.

3.1 MCI-c vs MCI-nc

MCI-c is the group that goes on to convert to AD in any of their subsequent follow-ups. The maximum span for this can be upto 4 years.

MCI-nc is the group that stays stable in all subsequent follow-ups.

Note that the patients in both groups **do not** have the same follow-ups - it is highly possible some patients in MCI-nc have much fewer follow-ups that MCI-c patients and have just not been detected as converters.

3.1.a Hyper-parameter search

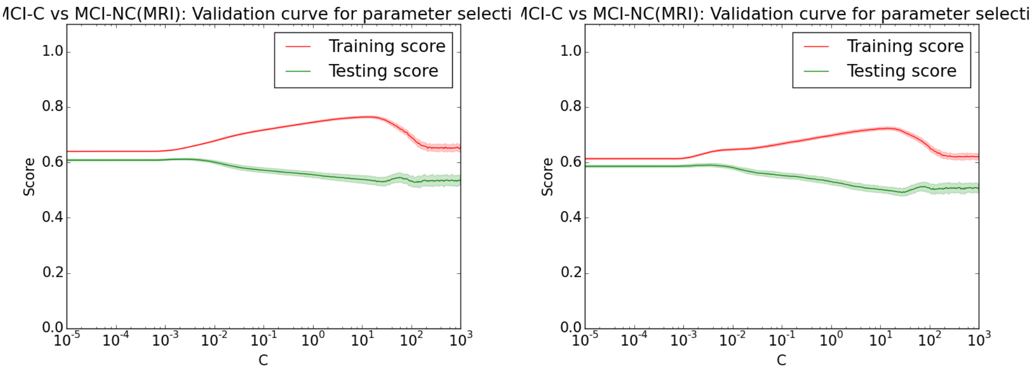

(a) Optimizing for ROC-AUC (b) Optimizing for accuracy

Figure 16: Hyper-parameter search using MRI-based features

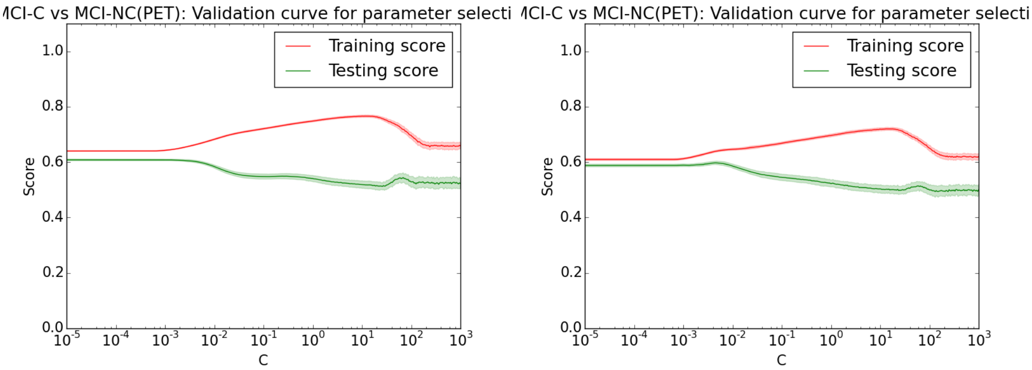

(a) Optimizing for ROC-AUC (b) Optimizing for accuracy

Figure 17: Hyper-parameter search using PET-based features

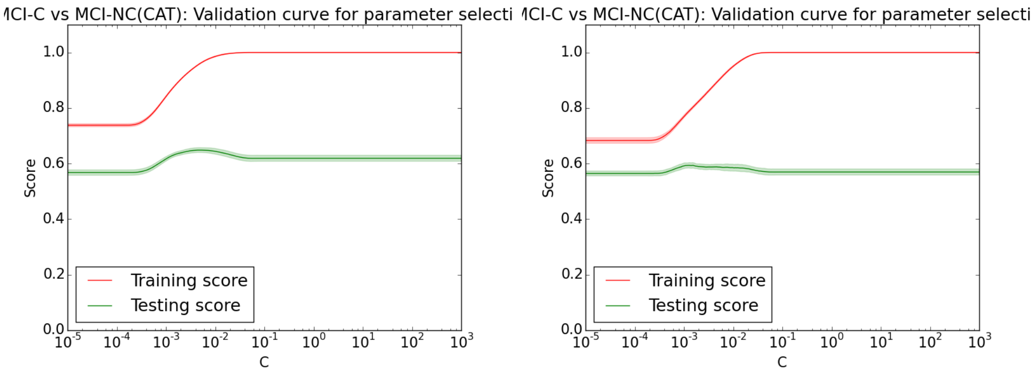

(a) Optimizing for ROC-AUC (b) Optimizing for accuracy

Figure 18: Hyper-parameter search using conCATenated features

3.1.b Classification results

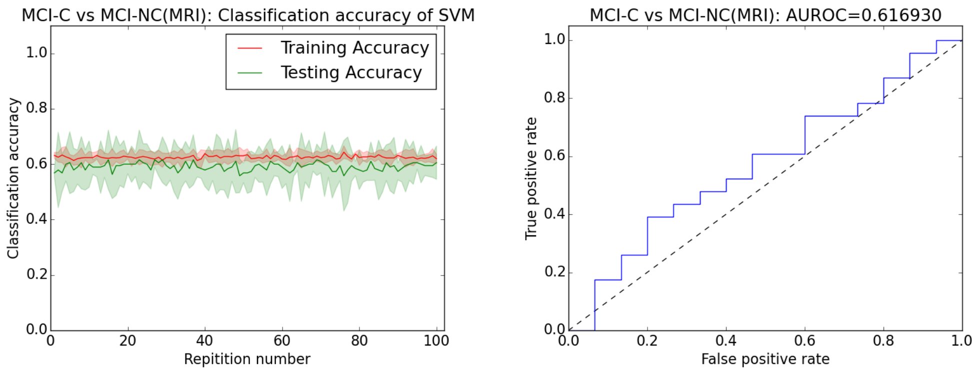

(a) Classification accuracy (b) ROC curves

Figure 19: Classification results using MRI-based features

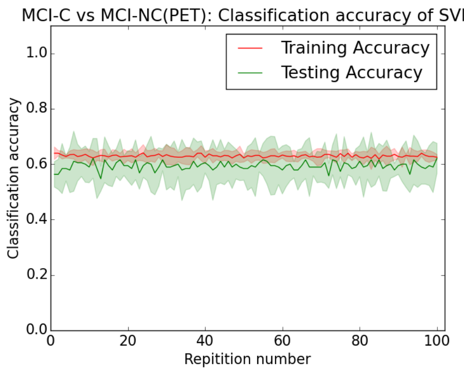

(a) Classification accuracy

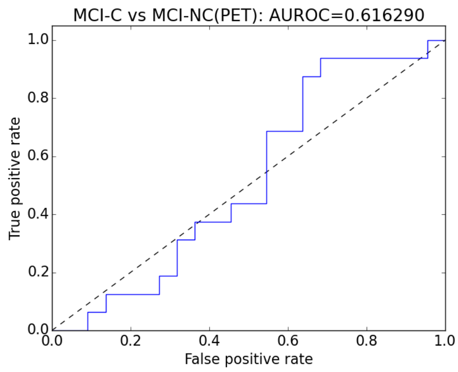

(b) ROC curves

Figure 20: Classification results using PET-based features

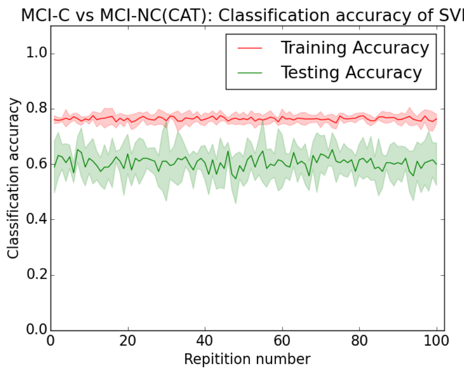

(a) Classification accuracy

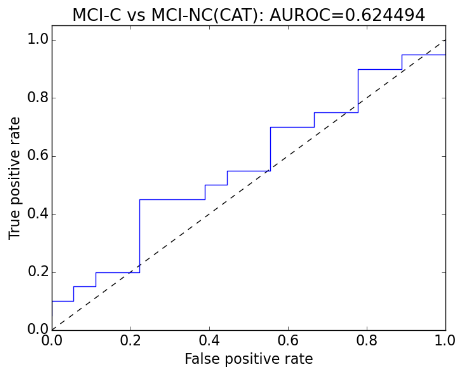

(b) ROC curves

Figure 21: Classification results using CAT-based features

3.1.c State of the Art

Zhang multi-modal multi-kernel:

MRI: 62%
PET: 63.9%
CSF: 51.8%
CONCAT(all three): 65.4%
Proposed: 73.9%

3.2 NL vs MCI

3.2.a Hyper-parameter search

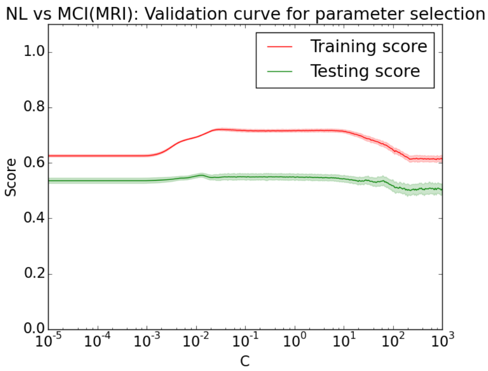

(a) Optimizing for ROC-AUC

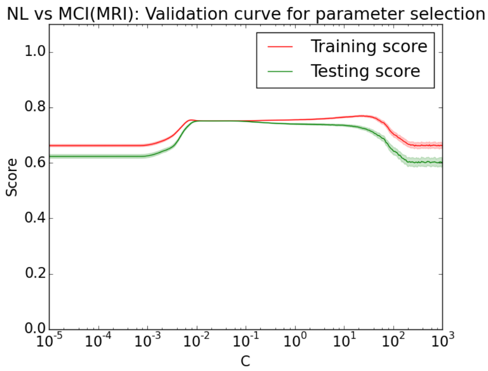

(b) Optimizing for accuracy

Figure 22: Hyper-parameter search using MRI-based features

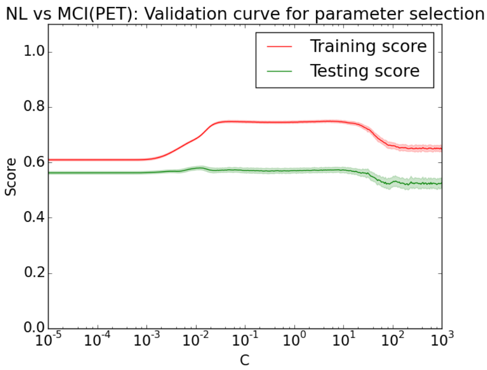

(a) Optimizing for ROC-AUC

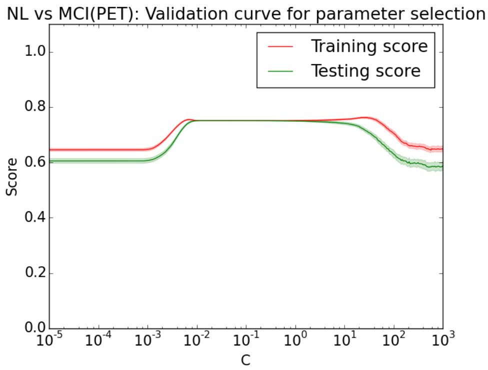

(b) Optimizing for accuracy

Figure 23: Hyper-parameter search using PET-based features

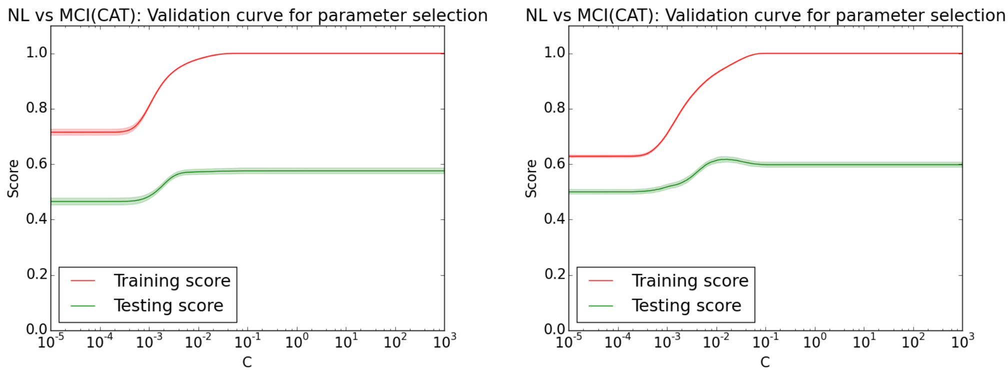

(a) Optimizing for ROC-AUC (b) Optimizing for accuracy

Figure 24: Hyper-parameter search using conCATenated features

3.2.b Classification results

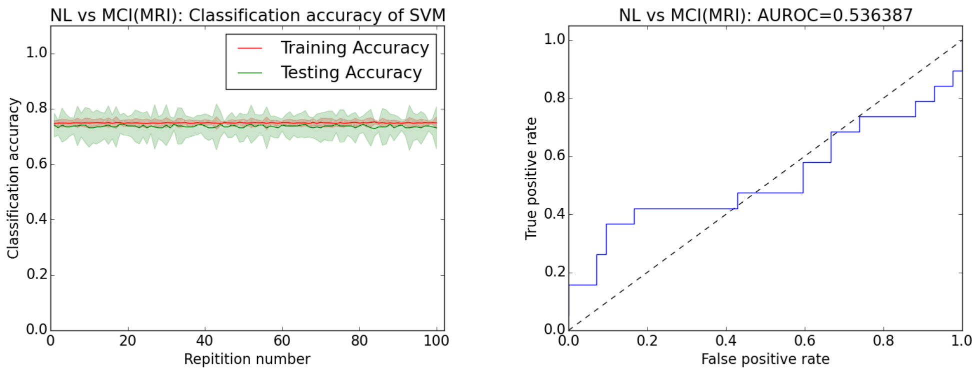

(a) Classification accuracy (b) ROC curves

Figure 25: Classification results using MRI-based features

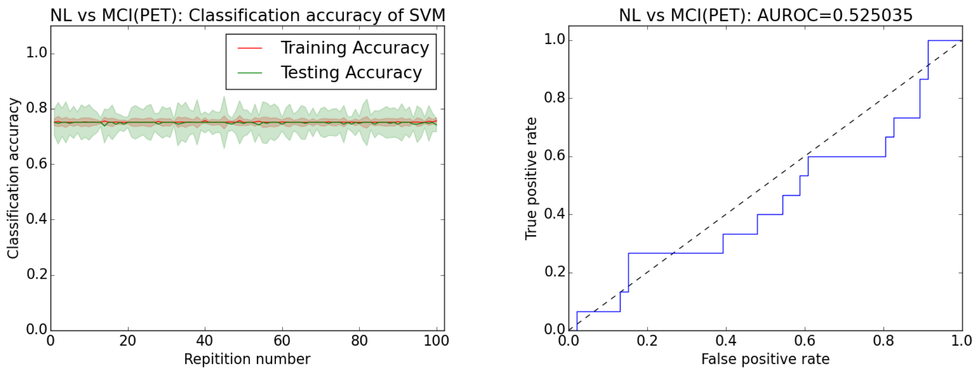

(a) Classification accuracy

(b) ROC curves

Figure 26: Classification results using PET-based features

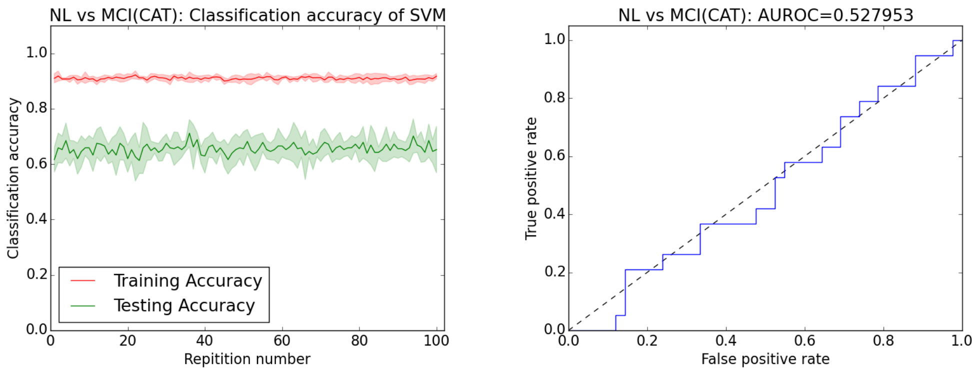

(a) Classification accuracy

(b) ROC curves

Figure 27: Classification results using CAT-based features

3.2.c State of the Art

Zhang multi-modal:

MRI: 72%
PET: 71.6%
CSF: 71.4%
ALL: 76.4%

3.3 NL vs AD

3.3.a Hyper-parameter search

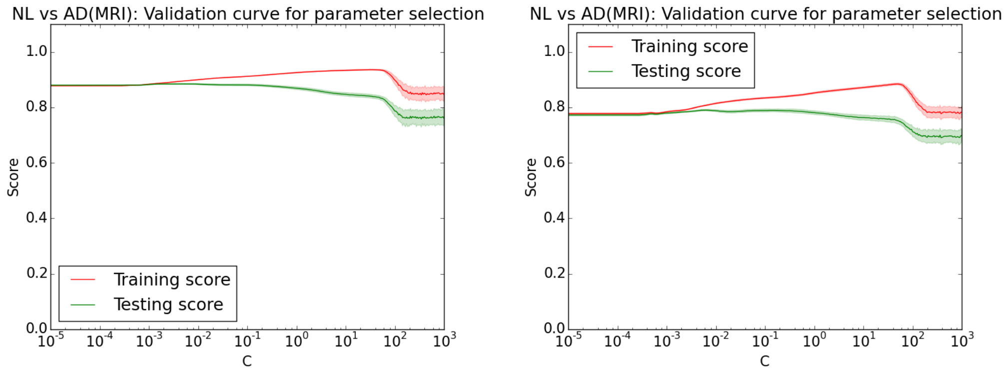

(a) Optimizing for ROC-AUC (b) Optimizing for accuracy

Figure 28: Hyper-parameter search using MRI-based features

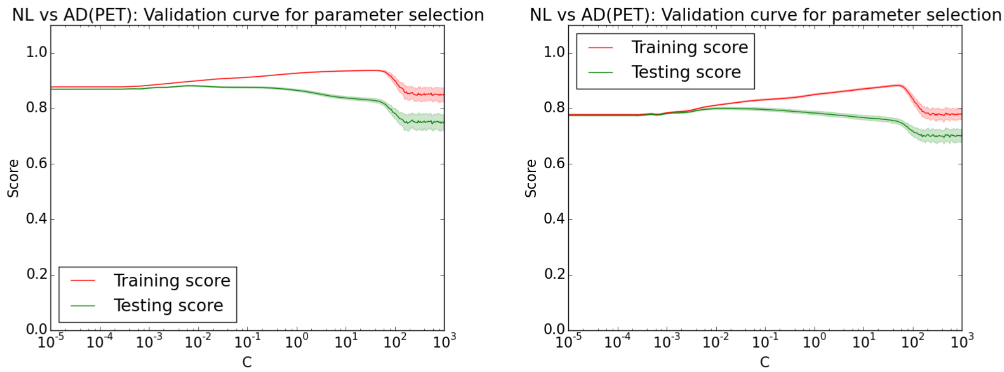

(a) Optimizing for ROC-AUC (b) Optimizing for accuracy

Figure 29: Hyper-parameter search using PET-based features

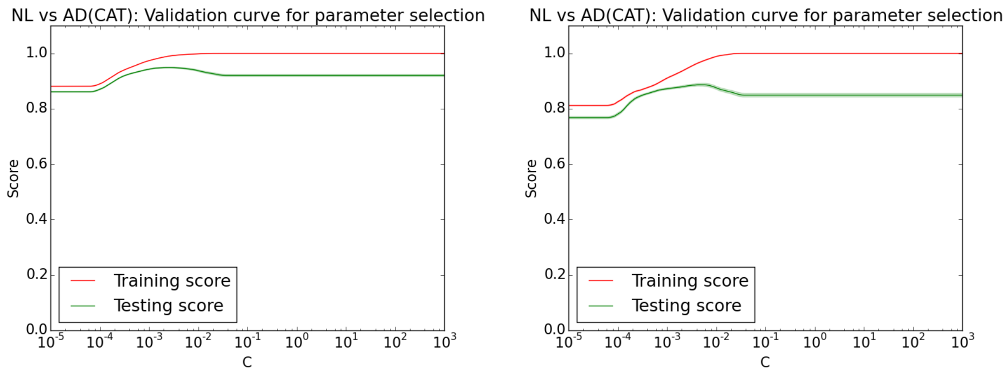

(a) Optimizing for ROC-AUC (b) Optimizing for accuracy

Figure 30: Hyper-parameter search using conCATenated features

3.3.b Classification results

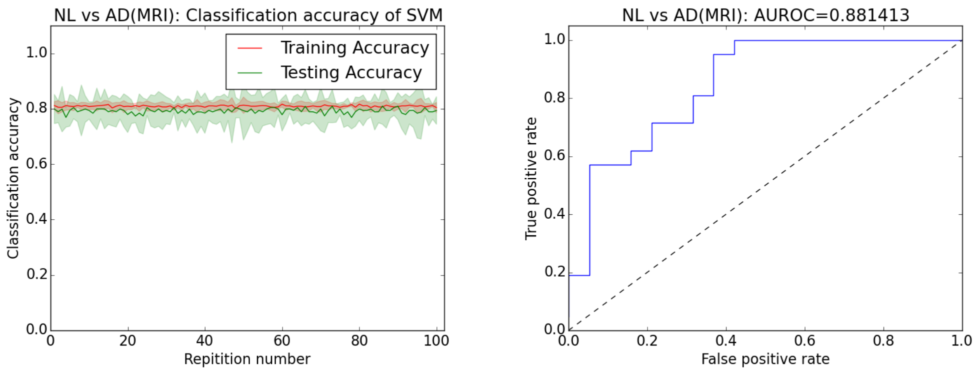

(a) Classification accuracy (b) ROC curves

Figure 31: Classification results using MRI-based features

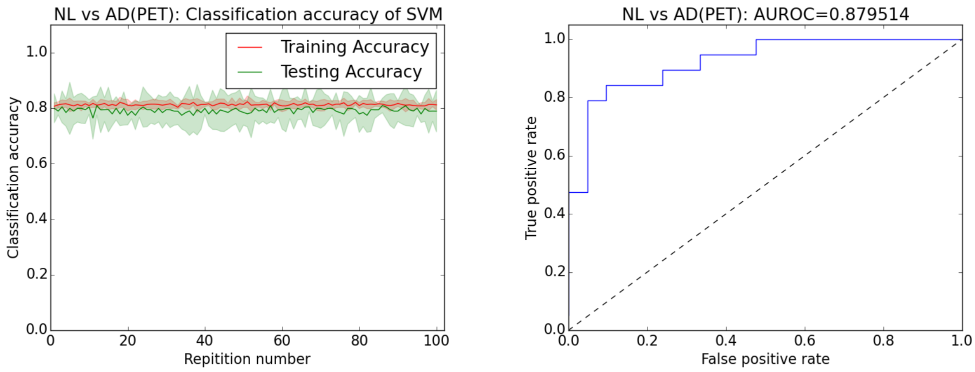

(a) Classification accuracy (b) ROC curves

Figure 32: Classification results using PET-based features

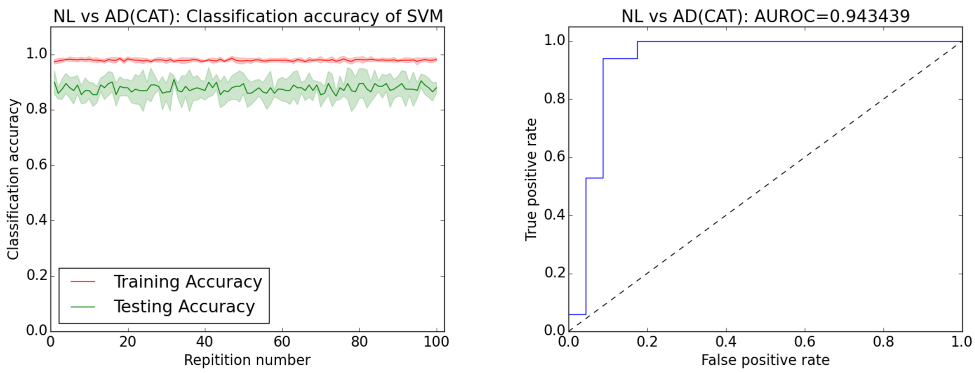

(a) Classification accuracy (b) ROC curves

Figure 33: Classification results using CAT-based features

3.3.c State of the Art

Zhang multi-modal kernel:

MRI: 86.2%
PET: 86.5%
CSF: 82.1%
ALL: 93.2%

3.4 MCI vs AD

3.4.a Hyper-parameter search

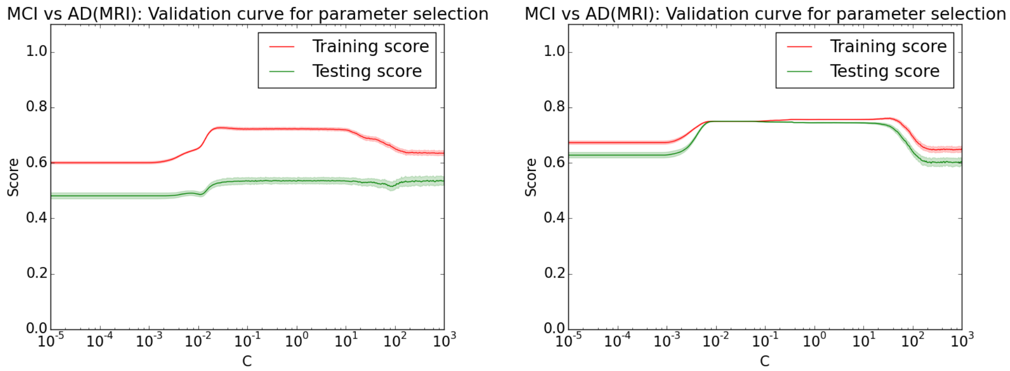

(a) Optimizing for ROC-AUC (b) Optimizing for accuracy

Figure 34: Hyper-parameter search using MRI-based features

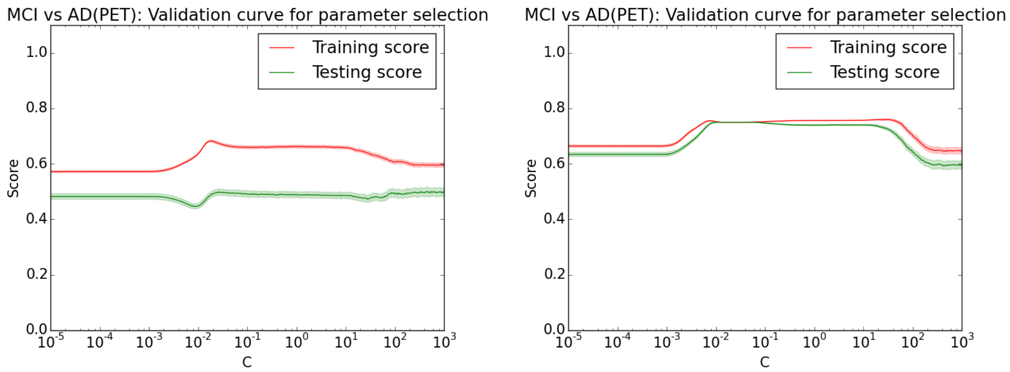

(a) Optimizing for ROC-AUC (b) Optimizing for accuracy

Figure 35: Hyper-parameter search using PET-based features

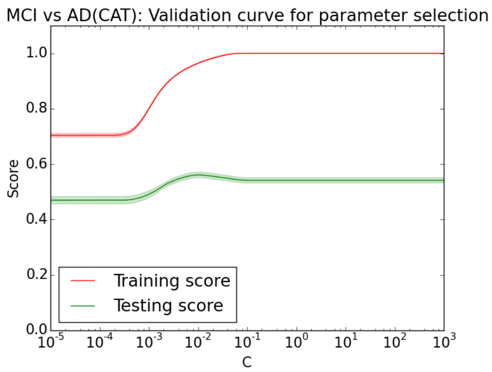

(a) Optimizing for ROC-AUC

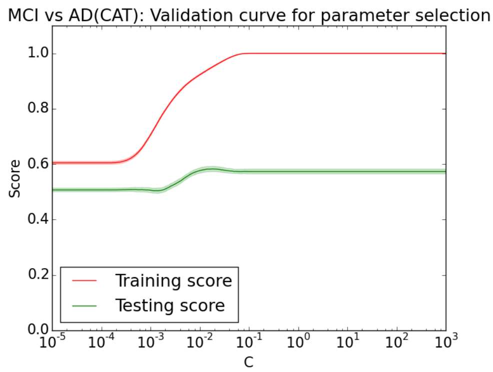

(b) Optimizing for accuracy

Figure 36: Hyper-parameter search using conCATenated features

3.4.b Classification results

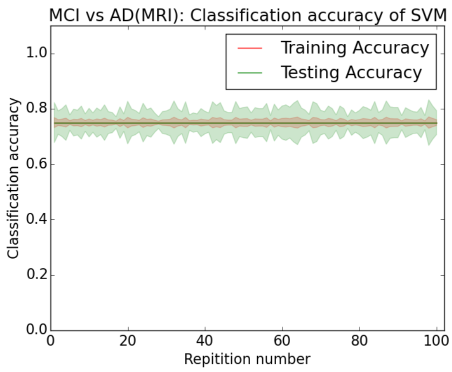

(a) Classification accuracy

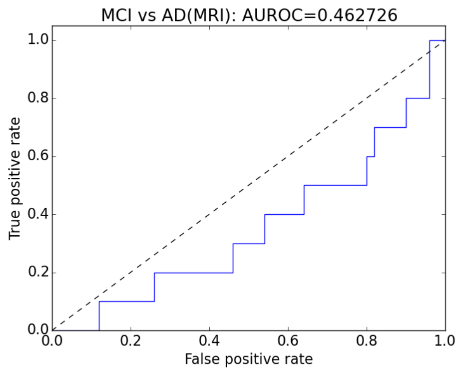

(b) ROC curves

Figure 37: Classification results using MRI-based features

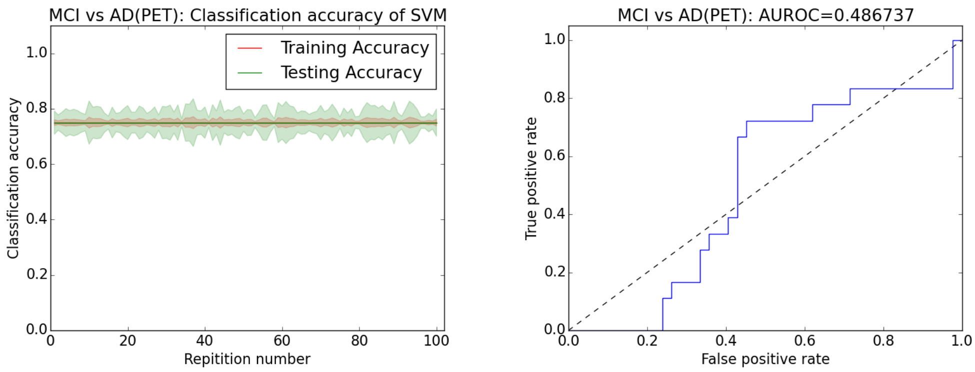

(a) Classification accuracy (b) ROC curves

Figure 38: Classification results using PET-based features

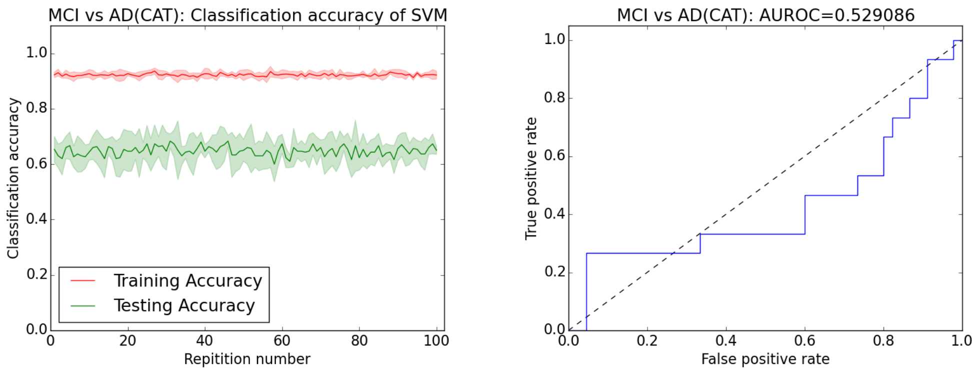

(a) Classification accuracy (b) ROC curves

Figure 39: Classification results using CAT-based features

3.4.c State of the Art